

Incorporating Storage as a Flexible Transmission Asset in Power System Operation Procedure

Mads Almassalkhi*, Yury Dvorkin[†], Jennifer Marley[‡], Ricardo Fernández-Blanco[†], Ian Hiskens[‡], Daniel Kirschen[†], Jonathon Martin[‡], Hrvoje Pandžić[§], Ting Qiu[†], Mushfiquar Sarker[†], Maria Vrakopoulou[‡], Yishen Wang[†], Mengran Xue[¶]

* School of Engineering, University of Vermont, Burlington, VT, USA

[†] Department of Electrical Engineering, University of Washington, Seattle, WA, USA

[‡] Department of Electrical Engineering and Computer Science, University of Michigan, Ann Arbor, MI, USA

[§] Faculty of Electrical Engineering and Computing, University of Zagreb, Zagreb, Croatia

[¶] Washington State University, Pullman, WA, USA

Abstract—Managing uncertainty caused by the large-scale integration of wind power is a challenge in both the day-ahead planning and real-time operation of a power system. Increasing system flexibility is the key factor in preserving operational reliability. While distributed energy storage is a promising way to increase system flexibility, its benefits have to be optimally exploited to justify its high installation cost.

Optimally operating distributed energy storage in an uncertain environment requires decisions on multiple time scales. Additionally, storage operation needs to be coordinated with the scheduling and dispatching of conventional generators. This paper proposes and demonstrates a three-level framework for coordinating day-ahead, near real-time and minute-by-minute control actions of conventional generating units and distributed energy storage. A case study illustrates the interactions between the three levels and the effectiveness of this approach both in terms of economics and operational reliability.

Index Terms—Power system operation, energy storage, uncertainty, unit commitment.

I. INTRODUCTION

A. Motivation and Literature Overview

The fast growing amount of variable and uncertain renewable generation capacity increases the need for flexibility in power system operation. Flexibility can be defined as the ability of the system to deploy resources on different time scales to respond to contingencies and actual or anticipated changes in net load, e.g. the difference between the actual load and the load served by uncontrollable generation. Besides conventional controllable generation, sources of flexibility include transmission switching, FACTS devices, demand response and energy storage. The research presented in this paper is focused on increasing the system flexibility by utilizing storage assets distributed across the power system, which is in line with the objectives of power system operators worldwide. In its Research and Development Roadmap 2013-2022, ENTSO-E

commits to research on the use of storage technologies to improve the planning and operation of transmission networks [1]. In the United States, the Department of Energy has embarked on an ambitious research program to stimulate research on storage technologies and integration [2]. Some US states and utilities have introduced energy storage mandates and incentives. For example, Decision 13-10-040 of the California Public Utilities Commission set a target of 1,325 MW of energy storage to be procured by investor-owned utilities before 2020 [3]. This decision led the California Independent System Operator to address the following issues facing its stakeholders: (i) expanding the revenue opportunities, (ii) reducing the cost of connecting storage units to the grid, and (iii) setting policies and processes to increase certainty [4]. In its 2030 Power System Study, ISO New England considers several generic scenarios that include 1 to 5 GW of newly installed storage [5]. In a study of current energy storage models, MISO acknowledges that they fail to capture the benefits that batteries can provide in the ancillary services market [6]. Finally, a study conducted by PJM concludes that storage could reduce the cost of congestion by \$9.5 million on a specific transmission line [7].

This industrial, regulatory and governmental interest in energy storage is accompanied by academic research on new approaches to the operation and integration of storage into existing power systems. For example, Monroy and Christie [8] investigated the effects of energy storage on the operational planning of a thermal power system. These simulations show that, for low penetration of wind energy, the optimal scheduling of storage is mostly determined by the load variations, resulting in daily cycles of storage operation. However, as the proportion of wind generation increases, storage operation stops exhibiting patterns.

Li and Hedman [9] studied the interplay between conventional generators and storage units using a stochastic unit commitment program. Similarly, Bruninx *et al.* [10] calculated the value provided by energy storage when scheduled using deterministic, stochastic and interval unit commitment algorithms. Both studies show that for high wind penetration

This work was supported in part by the ARPA-E Green Electricity Network Integration (GENI) program of the US Department of Energy under project DE-FOA-0000473.

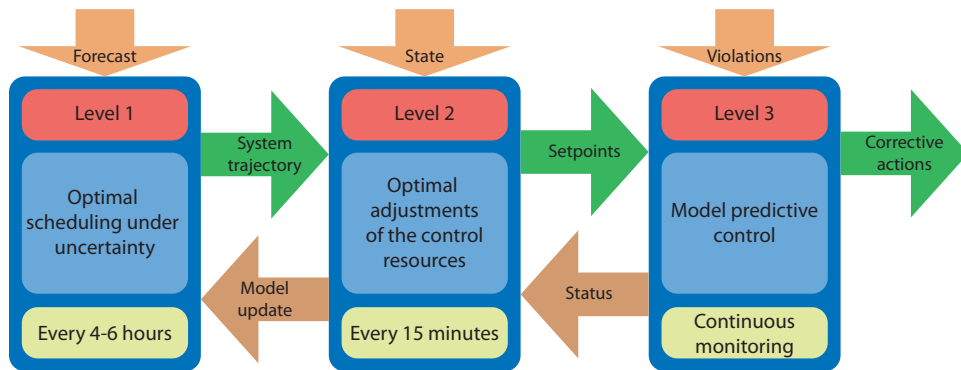


Figure 1. Structure of the proposed three-level operating framework.

levels energy storage reduces the system-wide operating cost and increase the capacity factor of conventional generators.

B. Proposed Framework

The aim of the research project described in this paper was to investigate how the flexibility provided by energy storage can be used to optimize the operation of power systems with a substantial portion of renewable generation. Distributed energy storage makes possible spatio-temporal arbitrage, i.e. the positioning of energy at strategic locations in the transmission network for consumption at a later time or further transmission when the network is less congested. In addition, distributed energy storage can be used for real-time system balancing, and post-contingency corrective actions. Fig. 1 illustrates the three-level framework that was developed to support all these applications on time scales that are appropriate for each of them.

Level 1 schedules generating units and energy storage over a 36-hour horizon every 4-6 hours, or more frequently if the actual renewable generation deviates significantly from the forecast. Because of the large number of binary variables that it must consider, Level 1 models transmission constraints using a linear (DC) model.

The generation and storage schedule produced by Level 1 represents an optimal system trajectory, which specifies for each time interval the output of each generator and the energy to be charged or discharged by each storage unit. This trajectory is passed on to Level 2, which assesses the actual conditions of the system every 15 minutes and updates the generation and storage schedules accordingly. In essence, Level 2 refines the decisions made by Level 1, taking into account the actual evolution of the system state. Level 2 incorporates a multi-period AC-OPF that is extended to capture the temporal coupling of storage. It uses a 4-hour optimization horizon with a 15-minute resolution. The storage state-of-charge values at the end of the 4-hour optimization horizon are set to match the Level 1 trajectory. This ensures that Level 2 maintains a balance between real-time conditions and the longer-term forecast.

Level 3 continuously monitors the system to detect violations of operating limits caused by contingencies or un-

expected changes in load or generation. It determines and implements corrective actions throughout the system using model predictive control.

Three events trigger a re-run of Level 1:

- 1) The availability of an updated forecast of renewable generation. We assume this happens every 4-6 hours, which is thus the longest time period between two Level 1 runs.
- 2) Level 2 detects an excessive discrepancy between the actual system state and the system trajectory calculated by Level 1. Such a discrepancy would be the result of a significantly inaccurate forecast of renewable generation.
- 3) Level 3 has implemented corrective actions to handle an overload or other contingency. Once the system has been stabilized, Level 1 is re-run using an updated list of available generating units and transmission branches.

II. DESCRIPTION OF THE THREE LEVELS

A. Level 1

Level 1 schedules the charging and discharging of energy storage alongside the commitment of conventional generating units, while taking into account transmission constraints. Our implementation is based on a combination of the 3BIN_MINUPDOWN and 3BIN_SUC Unit Commitment (UC) formulations from [11].

Adding storage to a conventional UC model results in the following nodal power balance equations:

$$\sum_{i \in \mathcal{G}_i} P_{g,i}(t) + W_i^{\max}(t) + \sum_{l \in \mathcal{L}} I_{il} P_l(t) + D_i(t) \eta^D = d_i(t) + \frac{C_i(t)}{\eta^C}, \forall i, \forall t \quad (1)$$

where the first term on the left-hand side is the sum of power outputs of generators, $P_{g,i}(t)$, at bus i (set \mathcal{G}_i) and time t ; the second term is the wind power available at bus i and time t ; the third term represents power flows through lines incident to bus i , where I_{il} is the line-bus incidence matrix and $P_l(t)$ is the directed line flow through line l (set \mathcal{L}) at time t ; the last term represents the energy discharged from the storage connected to bus i , where $D_i(t)$ is the discharging power of the storage and η^D is the storage discharging efficiency. On

the right-hand side, $d_i(t)$, is the overall load at bus i , $C_i(t)$ is the charging power of the storage connected to bus i and η^C is the storage charging efficiency.

The following constraint keeps track of the storage state-of-charge ($soc_i(t)$):

$$soc_i(t) = soc_i(t-1) + C_i(t) - D_i(t), \forall i, \forall t \quad (2)$$

Minimum (soc_i^{\min}) and maximum (soc_i^{\max}) state-of-charge, charging (C_i^{\max}) and discharging (D_i^{\max}) limits are imposed as follows:

$$soc_i^{\min} \leq soc_i(t) \leq soc_i^{\max}, \forall i, \forall t \quad (3)$$

$$0 \leq C_i(t) \leq C_i^{\max}, \forall i, \forall t \quad (4)$$

$$0 \leq D_i(t) \leq D_i^{\max}, \forall i, \forall t \quad (5)$$

The interested reader is referred to [12] for a complete UC model including energy storage.

Level 1 UC needs to be uncertainty-aware in order to provide sufficient generator and storage dispatch options for Level 2. The uncertainty on renewable generation at the day-ahead stage may be incorporated using a stochastic [13], robust [14], interval [15], improved interval [16] optimization, or an *ad hoc* reserve rule.

B. Level 2

Level 2 solves an AC-Optimal Power Flow (AC-OPF) problem using a successive linearization method. The details of this algorithm are summarized in Fig. 2. It is based on the traditional AC-Quadratic Program OPF (AC-QP OPF) solution method described in [17]. As the physical properties of storage devices introduce temporal coupling over the optimization horizon, the traditional OPF presented in [17] is modified to be a multiperiod OPF with a 4-hour horizon. The method begins by solving an AC-power flow at each time period in the Level 2 horizon using the initial generator, storage and wind schedules received from Level 1. Using the updated total system losses and line flows from the power flow, a simple QP is then solved that seeks to minimize the total quadratic cost of conventional generation while satisfying control variable limits and power balance throughout the network. The details of the QP solved can be found in Section II.B of [18]. In this QP, the total system power flow losses, $P^{\text{loss}}(t)$, are used to update the system-wide power balance constraint in the OPF horizon:

$$\sum_{i \in \mathcal{G}} P_{g,i}(t) - \sum_{i \in \mathcal{S}} r_i(t) + \sum_{i \in \mathcal{W}} (W_i^{\max}(t) - P_{w,i}(t)) = \sum_{i \in \mathcal{D}} d_i(t) + P^{\text{loss}}(t), \forall t \quad (6)$$

where all notations used in (1) have the same definition; $r_i(t) = C_i(t) - D_i(t)$ is the net storage active power injection at bus i ; $W_i^{\max}(t)$ is the available wind at bus i ; $P_{w,i}(t)$ is the wind curtailment at bus i ; and $d_i(t)$ is the active power demand at bus i . Sets \mathcal{G} , \mathcal{S} , \mathcal{W} , \mathcal{D} denote conventional generators,

storages, wind farms, and loads. Additionally, a linearized line flow constraint of the form

$$f_{i-j}^0 + \sum_{k \in \mathcal{G}} a_{i-j,k} (P_{g,k} - r_k - P_{w,k} - P_{g,k}^0 + r_k^0 + P_{w,k}^0) \leq f_{i-j}^{\max} \quad (7)$$

is added to the QP for each line $i-j$ whose active power flow, f_{i-j}^0 , exceeds its maximum flow limit f_{i-j}^{\max} . This way, the subset of lines for which line flow constraints must be included is relatively small, compared to the set of all lines in the network. In the previous equation, the superscript 0 quantities are results from the power flow. The $a_{i-j,k}$ coefficients are the line flow sensitivity factors computed offline, which reflect how the flow on line $i-j$ changes with a 1 p.u. change in generation at bus k .

After this first QP-power flow iteration, the net of storage charging and discharging for each device is used to set its status to either charging or discharging. This status is then enforced in the QP by fixing either its discharging or charging limit to 0. Doing so prevents simultaneous charging and discharging of storage devices in the final solution. The QP-power flow iterations then repeat, updating the (dis)charging status of each storage device after each QP solution, as well as the total system losses in (6) and the line flows in (7) after each power flow. The algorithm continues until two criteria are met. First, the QP and power flow results agree within a specified tolerance. Second, there are no overloaded lines in the power flow solution. When both criteria are satisfied, the final solution produced by Level 2 is an AC-feasible, optimal solution.

C. Level 3

A model-predictive control formulation is utilized by Level 3 to ensure reliable operation of the system. At each update of the State Estimator, device and operational limits are compared to the current system states. In the case of a limit violation, corrective measures are taken to guide the system back toward a secure operating condition. To determine these corrective actions, Level 3 sets up and solves a multi-period quadratic program (QP) predicting the system behavior at each minute over the next 15 minutes. The control actions identified for the first period are implemented on the actual network. At the start of the next minute, the new system conditions resulting from the applied control actions are retrieved from the State Estimator. If limit violations persist, the process is repeated; otherwise the system returns to normal operating procedures following the schedule determined by Level 2.

To capture the short-term flexibility inherent in electric power systems, Level 3 applies a linearized temperature model to transmission lines. By modeling line temperatures which are driven by losses and penalizing thermal overloads which cause unacceptable line sag, short-term power flow overloads are permitted immediately following contingencies. Stopping conditions ensure that any thermal overloads are relieved by the end of the prediction horizon. The model describing line losses and temperatures is presented as follows:

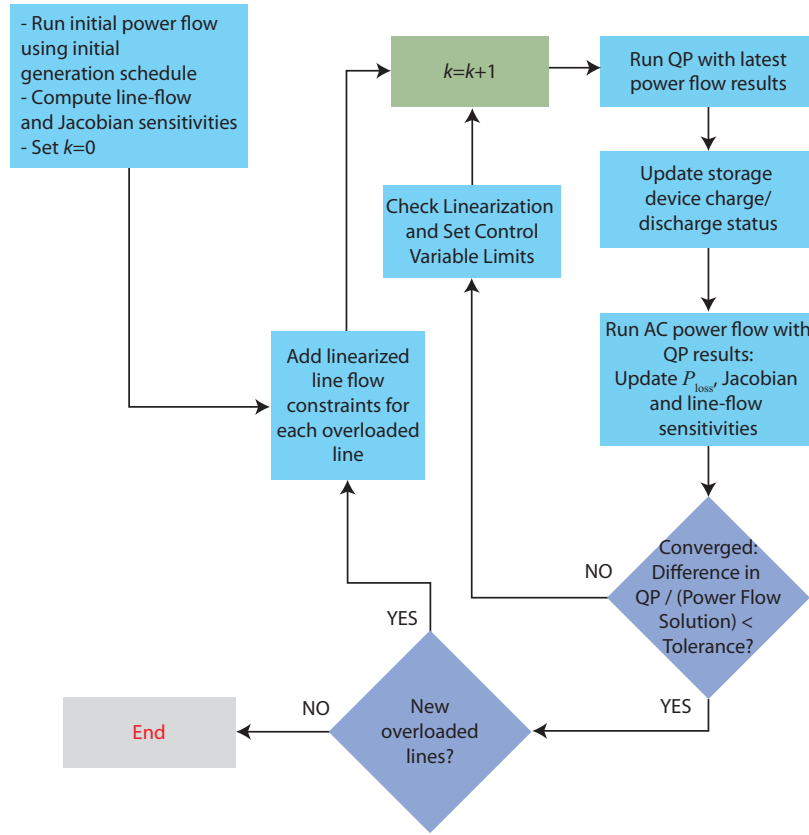


Figure 2. Level 2 AC-QP OPF Solution Method.

$$0 = \theta_{i,j}^+(t) - \theta_{i,j}^-(t) - \theta_{i,j}(t) \quad (8)$$

$$0 = \theta_{i,j}^+(t) - \theta_{i,j}^-(t) - \sum_{s=1}^S \theta_{i,j,s}^{\text{PW}}(t) \quad (9)$$

$$0 = \frac{x_{i,j}^2}{r_{i,j}} f_{i,j}^{\text{loss}}(t) - \Delta\theta \sum_{s=1}^S \alpha_{i,j,s} \theta_{i,j,s}^{\text{PW}}(t) \quad (10)$$

$$\Delta T_{i,j}(t+1) = \tau_{i,j} \Delta T_{i,j}(t) + \rho \Delta f_{i,j}^{\text{loss}}(t) + \delta_{i,j} \Delta d_{i,j} \quad (11)$$

$$\Delta \hat{T}_{i,j}(t) = \max \{ \Delta T_{i,j}(t), 0 \} \quad (12)$$

Equation (8) relates the voltage angle difference and the relaxation of its absolute value across the line connecting buses $i - j$ at time t . Equation (9) relates the absolute value relaxation of phase angle difference to an S -segment piecewise-linear model. Equation (10) uses the S -segment model of phase angle difference with segment width $\Delta\theta$ to build a piecewise-linear model of losses. The terms r_{ij} and x_{ij} represents the series resistance and reactance of the line. Equation (11) describes how losses affect line temperatures. Here, $\Delta T_{i,j}$ is the temperature difference between the line and its thermal rating, $\Delta f_{i,j}^{\text{loss}}$ is the difference between losses and the losses realized when the line is at its thermal rating, and $\Delta d_{i,j}$ describes any fluctuations in the ambient temperature and solar heat gain on the line. The coefficients $\tau_{i,j}$, ρ and

$\delta_{i,j}$ are determined based on line conductor specifications. Equation (12) defines the positive line temperature overloads penalized in the objective function based on the modelled line temperatures.

The multi-period QP solved by Level 3 penalizes deviations from the optimal Level 2 operating schedule in its objective and enforces device limits while modelling the system behavior through the linear constraints. These constraints include a power flow description, a piecewise-linear model of losses, a model of line temperature behavior, a model of storage charging/discharging and state-of-charge, power shedding capabilities for load and renewables, and a ramp-rate limited model of controllable generation. The derivation and discussion of these models is available in [19] and a presentation of the full QP formulation is available in [20].

D. Interactions between the Three Levels

The interface between Level 1 and Level 2 depends on clock time and deviations, as shown in the upper part of Fig. 3. A significant deviation occurs when the cumulative error on the wind and load forecasts or the deviation between the planned and actual dispatch decisions exceeds a given threshold. Level 1 dispatch decisions are x, g, l, c, d, s , representing the on/off generator statuses, generator outputs, line flows, storage charging, discharging, and state-of-charge, respectively. The corresponding Level 2 variables are denoted by an asterisk. If no threshold is crossed, Level 2 runs every

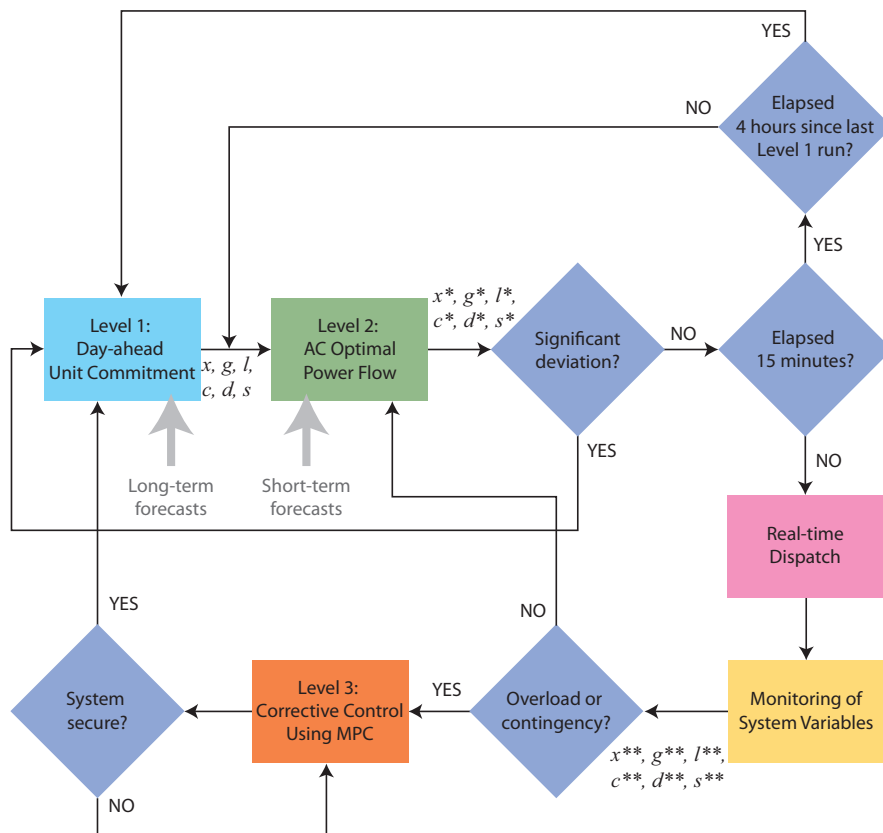


Figure 3. Interaction between the three levels.

15 min and Level 1 every 4 hours, since we assume an updated forecast is available every 4 hours.

In actual system operation, the real-time dispatch variables (denoted with two asterisks) are constantly monitored. In case an overload or contingency is detected, Level 3 is called upon to relieve the overloads and bring the system back to a secure state. As soon as the system is brought back to the secure state, Level 1 is initiated to provide a new system trajectory.

III. CASE STUDY

A. Data

The case study is based on the IEEE Three-Area Reliability Test System [21], which comprises 73 buses, 120 transmission lines, 96 generating units, 19 wind farms, 51 loads, and 36 hourly time intervals. Network data can be found in [21]. The capacities of the transmission lines were reduced to 80% of their original values. Demand and controllable generation data was taken from [11]. Wind data, including the location, capacity, and utilization factor, are given in [12]. We use a $(3 + 5)\%$ reserve policy, but set the reserve component accounting for load uncertainties to 2%. Finally, energy storage locations and sizes are optimized using the technique described in [12]. Table I summarizes their optimal locations, maximum energy state-of-charge, maximum charging/discharging rates, and the initial state-of-charge (based on their operation on the previous day) of the storage units. We also assume that the round-trip efficiency is 0.81 for all energy storage devices.

TABLE I. ENERGY STORAGE DATA.

Bus	soc_i^{\max} (MWh)	C_i^{\max}, D_i^{\max} (MW)	$soc_i(0)$ (MWh)
116	303	41	164.02
117	117	17	65.79
119	247	36	144.00
121	629	93	371.99
202	143	22	87.99
208	76	12	45.48
223	354	54	213.99
325	243	41	157.69

B. Demonstration

This section illustrates the mechanics of the proposed three-level framework. Fig. 4 shows the evolution of the system in three plots spanning a 36-hour window. These plots are updated each time levels 1 and 2 are run. The upper plot represents (i) the total system demand, (ii) the total power output of the generating units after solving the Level 1 optimization, and (iii) the total power output of the conventional generators after solving the Level 2 optimization. The middle plot shows the total long-term wind forecast and the total wind spillage after solving the optimization for levels 1 and 2. Finally, the lower plot shows the total energy state-of-charge after solving the optimization for Levels 1 and 2. The demo operates on a 15-min time interval. We focus our explanation on the actions and the subsequent results for each operating time interval. A

full video of this demonstration can be downloaded from [22].

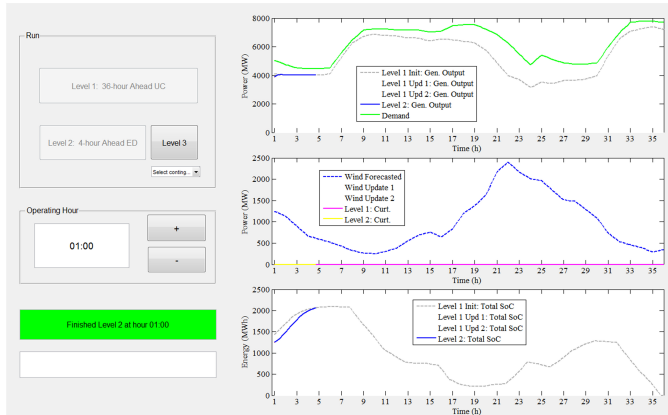


Figure 4. Graphic display of the demo after hour 01:00.

- Hour 01:00
 - Run Level 1 to obtain the schedule and storage decisions for the next 36 hours with a 1-hour resolution.
 - Run Level 2 to obtain the economic dispatch and storage decisions for the next 4 hours with a 15-min resolution.
 - Fig. 4 shows the results after running both levels at this hour.
- Hour 01:15
 - Check if there are significant wind deviations. If so, re-run Level 1. Otherwise, run Level 2. At this time, the wind deviations are not significant.
 - Run Level 2 to obtain the actual dispatch for the next 15 min, as well as the economic dispatch and storage decisions for the next 4 hours.
- Hours 01:30–03:45
 - The same actions and results as those provided at hour 01:15 apply at these hours.
 - Fig. 5 shows the results after hour 03:45. As previously stated, Level 1 should be re-run every 4 hours. The total wind deviation amounts 2.32% of the total load. We can also observe that a new long-term forecast has been updated in the middle plot of this figure for the remaining hours (shown in light blue). The realization of the overall conventional generation outputs, overall wind outputs and storage state-of-charge are shown in red in all three graphs.
- Hour 04:00
 - Run Level 1 because of the updated long-term wind forecast to obtain the updated schedule and storage decisions for the remaining hours of the time horizon.
 - Run Level 2 to obtain the updated economic dispatch and storage decisions for the next 4 hours.
- Hours 04:15–06:45
 - The same actions and results as those provided at hour 01:15 apply at these hours.

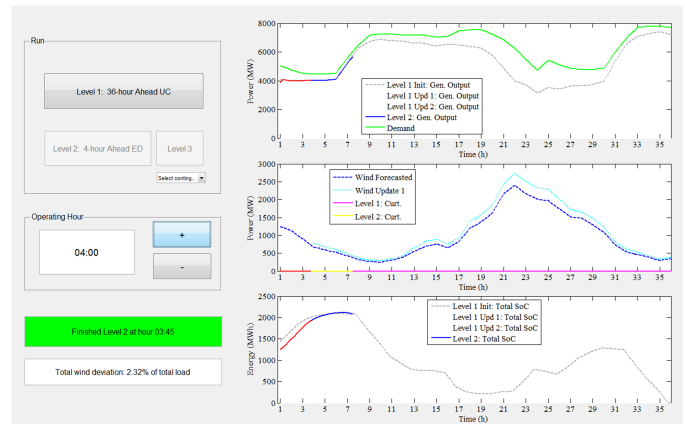


Figure 5. Graphic display of the demo after hour 03:45.

- Hour 07:00
 - A significant wind deviation is detected. The long-term wind forecast is updated and the Level 1 is re-run to update the schedule and storage decisions.
 - Run Level 2 to obtain the actual dispatch for the next 15 min, as well as the economic dispatch and storage decisions for the next 4 hours.
- Hours 07:15–09:15
 - The same actions and results as those provided at hour 01:15 apply at these hours.
- Hour 09:30
 - Check if there are significant wind deviations. If so, re-run Level 1. Otherwise, run Level 2. At this time, there are no significant deviations.
 - Run Level 2 to obtain the actual dispatch for the first 15 min, as well as the economic dispatch and storage decisions for the next 4 hours.
 - A contingency occurs on line 119. Level 3 is automatically triggered to obtain the corrective dispatch and storage decisions needed to mitigate the overload. The energy state-of-charge and the discharging rates for the ES devices are displayed in the two plots on the left-hand side of Fig. 6. On the right-hand side of this figure, the demo would provide plots representing the overloaded transmission lines if there were any.
 - Re-run Level 1 to obtain the updated schedule and storage decisions for the remaining hours of the time horizon.
- Hours 09:45–end
 - The same process is repeated.

C. IEEE-RTS-96 Results

The cost performance of the proposed three-level operating framework is compared to the benchmark using the data described in Section III-A. The benchmark includes two stages. The first stage solves the day-ahead deterministic unit commitment model, as presented in [11], using the 24-hour-ahead load and wind forecasts. The second stage performs an

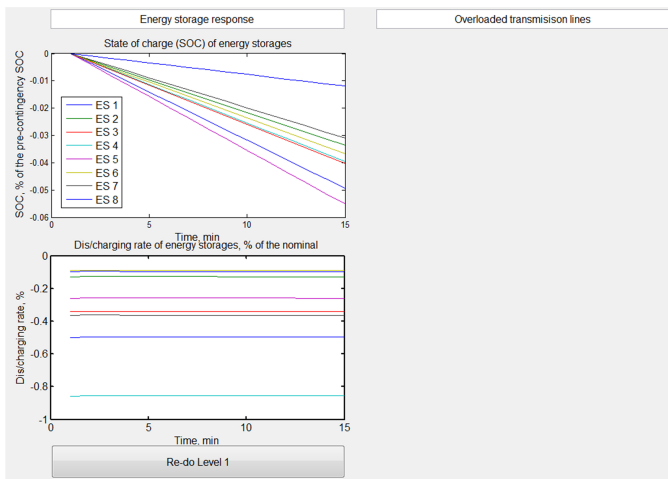


Figure 6. Graphic display of the demo after running Level 3 at hour 09:30.

hour-ahead re-commitment and re-dispatch subject to the day-ahead decisions and uses 1-hour-ahead forecasts. The second-stage decisions are then tested against the actual materialization of load and wind forecasts. The daily operating cost of the deterministic benchmark and the proposed three-level framework is calculated as the sum of the start-up and ex-post fuel costs of conventional generators without penalizing wind power generation spillage. The ex-post fuel cost was used to factor in the cost of corrective actions to mitigate real-time deviations from forecast conditions.

The daily operating costs without contingencies is \$2,109,811 for the benchmark case and \$2,068,037 for the three-level framework, thus leading to a saving of \$41,744 (1.98%). This saving consists of a \$33,451 reduction in fuel cost and a \$8,282 reduction in start-up cost. The reduction in start-up cost arises because generators belonging to groups U100, U155, and U400 do not have to be brought online.

If there is a contingency on line 119, as explained in Section III-B, the solution obtained with the benchmark is infeasible. On the other hand, the three-level framework mitigates the overloads caused by the contingency within 15 minutes. The post-contingency corrective actions increase the daily operating cost of the three-level framework by \$18,006 (0.87%).

IV. CONCLUSION

This paper proposes a novel three-level power system operating framework that incorporates the scheduling, and dispatch of distributed energy storage. This framework also supports the use of energy storage for post-contingency corrective actions. A case study shows that this framework can achieve a 2% cost savings as compared to a benchmark involving a more conventional operational practice.

The case study illustrates the importance of intra-day forecast updates (Level 1) and of the Level 1-2 interface in case of significant deviations from the forecast conditions. It also

shows the effectiveness of Level 3 in mitigating transmission line overloads within a given time limit, as well as the value of the interface between Level 3 and Levels 1 and 2 in mitigating the post-contingency operating cost.

REFERENCES

- [1] ENTSO-E, *Research & Development Roadmap 2013-2022 Writing History Again*, <http://tinyurl.com/phamk47>
- [2] US Department of Energy, *Grid Energy Storage*, Dec. 2013, <http://tinyurl.com/p2ullx6>
- [3] California Public Utilities Commission, *Decision Adopting Energy Storage Procurement Framework and Design Program*, October 2013, tinyurl.com/ovov4g7
- [4] California ISO, *Advancing and Maximizing the Value of Energy Storage Technology*, December 2014, tinyurl.com/qj2sfc3
- [5] ISO New England, *New England 2030 Power System Study*, February 2010, tinyurl.com/l4bmy8v
- [6] EPRI, *MISO Energy Storage Study Phase 1 Report*, November 2011, tinyurl.com/pcvm8gn
- [7] PJM Interconnection and Xtreme Power, *Energy Storage as a Transmission Asset*, 2012, tinyurl.com/pjh5bj9
- [8] C.A. Silva Monroy and R.D. Christie, "Energy storage effects on day-ahead operation of power systems with high wind penetration," in *Proc. of North American Power Symposium (NAPS)*, 2011, pp. 1–7.
- [9] N. Li and K.W. Hedman, "Economic assessment of energy storage in systems with high levels of renewable resources," *IEEE Trans. Power Syst.*, vol. 6, no. 3, Jul. 2015, pp. 1949–3029.
- [10] K. Bruninx, Y. Dvorkin, E. Delarue, H. Pandžić, W. D'haeseleer, D. S. Kirschen, "Coupling Pumped Hydro Energy Storage with Unit Commitment," *IEEE Trans. Sust. En.*, early access.
- [11] H. Pandžić, T. Qiu and D.S. Kirschen, "Comparison of state-of-the-art transmission constrained unit commitment formulations," in *Proc. of 2013 IEEE PES General Meeting*, 2013, pp. 1–5.
- [12] H. Pandžić, Y. Wang, T. Qiu, Y. Dvorkin, and D.S. Kirschen, "Near-optimal method for siting and sizing of distributed storage in a transmission network," *IEEE Trans. Power Syst.*, vol. 30, no. 5, Sep. 2015, pp. 2288–2300.
- [13] S. Takriti, J.R. Birge, and E. Long, "A stochastic model for the unit commitment problem," *IEEE Trans. Power Syst.*, vol. 11, no. 3, Aug. 1996, pp. 1497–1508.
- [14] D. Bertsimas, E. Litvinov, X.A. Sun, Z. Jinye, and Z. Tongxin, "Adaptive robust optimization for the security constrained unit commitment problem," *IEEE Trans. Power Syst.*, vol. 28, no. 1, Feb. 2013, pp. 52–63.
- [15] Y. Wang, Q. Xia, and C. Kang, "Unit commitment with volatile node injections by using interval optimization," *IEEE Trans. Power Syst.*, vol. 26, no. 3, Aug. 2011, pp. 1705–1713.
- [16] H. Pandžić, Y. Dvorkin, T. Qiu, Y. Wang, and D. Kirschen, "Toward cost-efficient and reliable unit commitment under uncertainty," *IEEE Trans. Power Syst.*, vol. PP, no. 99.
- [17] A. Wood, B. Wollenberg, and G. B. Sheble, *Power Generation, Operation and Control*, 3rd ed. New York: John Wiley and Sons, Inc., 2013.
- [18] J.K. Felder and I.A. Hiskens, "Optimal power flow with storage," in *Proc. of the 18th Power Systems Computation Conference*, 2014, pp. 1–7.
- [19] M.R. Almassalkhi and I.A. Hiskens, "Model-predictive cascade mitigation in electric power systems with storage and renewables – Part I: Theory and implementation," *IEEE Trans. Power Syst.*, vol. 30, no. 1, Jan. 2015, pp. 67–77.
- [20] M.R. Almassalkhi and I.A. Hiskens, "Model-predictive cascade mitigation in electric power systems with storage and renewables – Part II: Theory and implementation," *IEEE Trans. Power Syst.*, vol. 30, no. 1, Jan. 2015, pp. 78–87.
- [21] Reliability Test System Task Force, "The IEEE Reliability Test System—1996," *IEEE Trans. Power Syst.*, vol. 14, no. 3, Aug. 1999, pp. 1010–1020.
- [22] Demonstration video of the three-level operating framework, https://youtu.be/3_LPVsOL1fI